Proceedings of the Sixth International ASME Conference on Nanochannels, Microchannels and Minichannels
ICNMM2008
June 23-25, 2008, Darmstadt, Germany

ICNMM2008-62014

MICROCHANNEL FLUORESCENT MELTING CURVE ANALYSIS

David J Kinahan † *

Stokes Bio Ltd †
Shannon Arms
Henry Street
Limerick
Republic of Ireland

Tara M Dalton †‡

Mark R Davies †‡

Stokes Institute ‡
Dept. of Mechanical and Aeronautical Eng.
University of Limerick
Limerick
Republic of Ireland

ABSTRACT

In recent years, Fluorescent Melting Curve Analysis (FMCA) has become an almost ubiquitous feature of commercial quantitative PCR (qPCR) thermal cyclers. Here a microfluidic device is presented capable of performing droplet based Fluorescent Melting Curve Analysis within a microchannel. The device consists of modular thermally conductive blocks which can sandwich a microfluidic substrate. Opposing ends of the blocks are held at differing temperatures and a linear thermal gradient is generated along the microfluidic channel. Fluorescent measurements taken from a sample as it passes along the micro-fluidic channel permits fluorescent melting curves be generated. In this study we demonstrate the capability of measuring fluorescent melt curves from DNA passing through the device in a serial flow of sample plugs buffered by mineral oil.

1 INTRODUCTION

Many ailments have been found to have a genetic cause (1; 2). Of the methodologies with potential for wide-spread clinical application in the field of genomics, the polymerase chain reaction (PCR) has been found to have superior diagnostic accuracy compared with competing technologies such as the microgene array (3; 4; 5). The inherent ability of the PCR to allow analysis take place when only small genetic samples are available makes it particularly suitable to medical diagnostic application (6). Many research groups are undertaking work with the aim of developing high throughput Micro Total Analysis Systems (μTAS) (7) which will attenuate the remaining barriers that limit the potential of PCR; such as high reagent costs (4).

PCR micro-thermocyclers can be divided into two primary types; time domain (well based) PCR where the reaction is kept stationary and the temporally cycled between the different temperatures and space domain (flowing) PCR where the reaction is moved between zones of fixed temperature (7; 8).

Fluorescent Melting Curve Analysis (FMCA) (9) has been used to validate PCR assays and is an almost ubiquitous feature of commercial qPCR thermal cyclers (10). The thermodynamic stability of the PCR product is dependant on both its length and its base pair composition. Hence, samples of differing length and compositions will have differing melting temperatures (t_m). The addition of fluorescent double-stranded DNA (dsDNA) dye to a PCR assay allows measurement of each amplicon's melting temperature. FMCA involves continuously measuring the fluorescence of a PCR reaction as it is slowly heated to approximately $95°C$. At the sample's denaturation temperature, t_m, the dsDNA dye will suffer a drop in quantum efficiency. Hence, the t_m will be observed on the fluorescent-temperature (melting) plot as a sudden, non-linear, decrease in fluorescence.

The presence of dsDNA dye in many qPCR assays means that FMCA provides a fast, repeatable, closed tube end point analysis for these samples (11). However, it also has applications beyond quality control. When combined with appropriate

*Correspondence to david.kinahan@stokesbio.ie

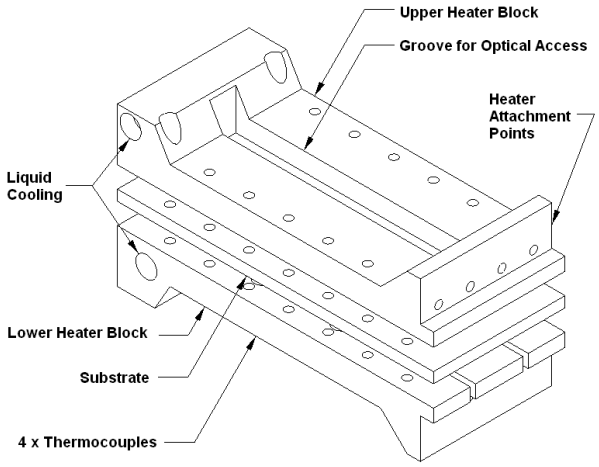

Figure 1. Exploded view of thermal blocks.

primer/probe selection melting curve analysis becomes an important tool in multiplex PCR (12). The melting curve method has also been used to detect single nucleotide polymorphisms (SNPs) (13; 14) in homozygous samples based on differences in t_m measured between wild-type and mutated samples. Where wild-type and mutated samples have almost identical $t_m s$, melting analysis can be applied to heterozygous samples to detect SNPs based on changes in the shape of the melting curves (14). A number of high resolution melting analysis machines have been developed specifically for applications in SNP detection (10).

Efforts have been made to develop Fluorescent Melting Curve Analysis for application on the micro-scale. Cibuzar et al applied a thermal gradient across a number of wells etched in a silicon substrate and measured fluorescence intensity in each well (15). Mao et al applied a linear thermal gradient across a series of parallel channels to perform FMCA (16). Sundberg et al performed heterozygous melting analysis on stationary samples in a custom microchannel (17), successfully taking measurements from volumes as low as 10nl. Dalton et al describes FMCA which takes place by applying a thermal gradient along a microchannel and continuously measuring the fluorescence of the sample as it passes along the channel (18). Dalton et al maintain the sample in a uniform light field by keeping the sample and optical detection system stationary relative to each other. Hence, only one sample may be analysed at a time. Here we describe a similar system, except in this case a serial flow of droplets, buffered by mineral oil, pass through a stationary non-homogenous light field.

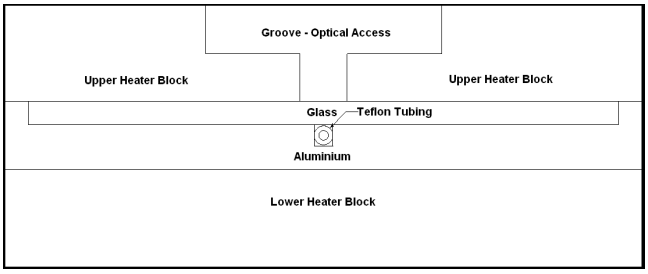

Figure 2. Cross Section (Detail) of Aluminium Substrate sandwiched by thermal blocks.

2 BIOLOGICAL MATERIAL

A PCR fragment was amplified from E. Coli. The plasmid vector pGEM-5Zf(+) (Promega) was used in conjunction with forward primer 5'- AGG GTT TTC CCA GTC ACG ACG TT-3' and a reverse primer 5'-CAG GAA ACA GCT ATG ACC-3' to produce a 240bp long fragment with a measured t_m of $90.9°C$. Primers were obtained from MWG Biotech (Ebersberg, Germany). Samples were amplified using LightCycler Faststart DNA Master SYBR Green I reaction mix (Roche) and thermocycled (with subsequent melting analysis) using the Applied Biosystems AB7900 thermocycler. Samples were then frozen at $-20°C$ before use. The temperature profile used for PCR amplification was made up of a pre-denaturation step ($95°C$ for $168s$) and 30 thermocycles, constituted of a denaturation step ($95°C$ for $10s$), an annealing step ($55°C$ for $10s$) and an extension step ($72°C$ for $15s$).

3 DESCRIPTION OF TEST RIG

3.1 Rig Design

The test rig consists of two aluminium heater blocks each of length 120mm, width 50mm and minimum thickness 10mm, designed to sandwich an interchangeable substrate [Fig. 1]. The sample channel is disposable Teflon FEP tubing (Upchurch Scientific) of OD 0.81mm and ID 0.405mm. The tubing is aligned within the test rig using an aluminium substrate. The substrate also serves to promote heat transfer between the rig thermal blocks and the tubing.

The substrate consists of an aluminium plate 3mm thick. Into the plate a recess 25mm wide and 1mm deep is machined in order to accommodate a borosilicate glass microscope slide (which acts as a cover plate). Additionally, a further groove 0.9mm deep and 0.8mm wide is machined into the substrate along its centre line. The substrate is then sprayed black. The disposable teflon tubing fits into this groove (an interference fit in order to promote heat transfer). The borosilicate glass slide is then placed in position over the tubing. The aluminium substrate is then sandwiched between the heater blocks and the assembly

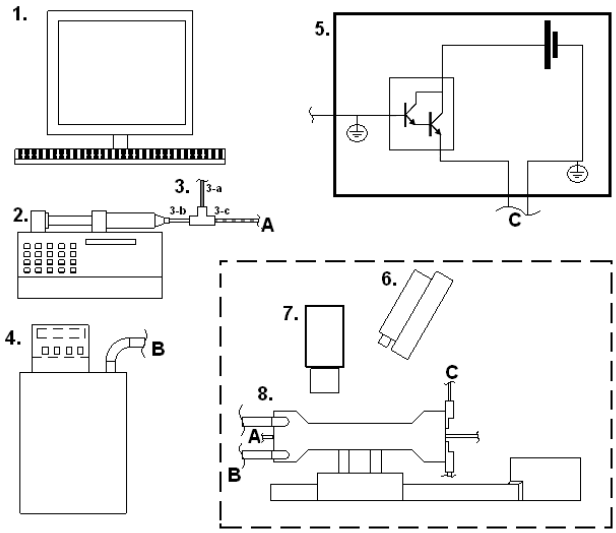

Figure 3. Schematic of experimental setup. 1. Computer for control/datalogging. 2. Syringe Pump. 3. T for droplet generation (3-a: Sample Port, 3-b: Carrier Fluid Port, 3-c: Outlet Port). 4. Heater bath for cooling. 5. Control circuit for heaters. 6. Excitation Laser. 7. Monochrome Camera. 8. Thermal Blocks. A-A, B-B and C-C indicate connections for wiring and tubing.

is bolted together.

The *Hot End* of the heater blocks are designed to be compatible with thick film resistors and darlington transistors within TO-220 standard packaging. The *Cold End* has a transverse, tapped bore for liquid cooling. The upper heater block has a groove milled to provide optical access to the substrate. The groove is 84mm long and 12mm wide, stepping to 2mm wide 2mm from its contact surface [Fig. 2]. The lower block has 4 thermocouples equally spaced along its centreline. The position of the thermocouples correspond to the optical access groove when the two blocks are mated together.

3.2 Heat Transfer in Test Rig

Due to the thermal conductivity of aluminium, and associated low Biot number of the thermal blocks at these dimensions, it is assumed that the temperature field across the thermal blocks is approximated by the one dimensional heat transfer equation. Assuming constant boundary conditions at the *hot end* and *cold end* of the thermal blocks, located at $x = 0$ and $x = L$ respectively, the temperature field of the blocks may be assumed to be:

$$T(x) = (T_h - T_c)\frac{x}{L} + T_c \qquad (1)$$

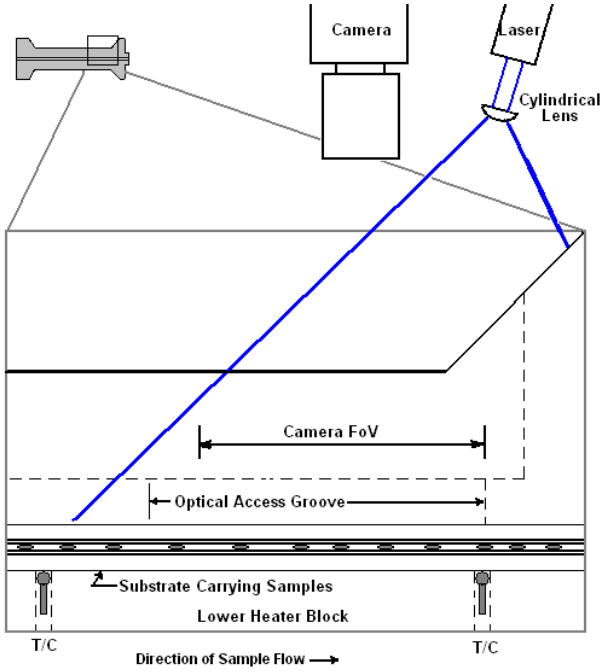

Figure 4. Schematic of the optical setup.

The temperature of any sample traversing the device will be dependant on its location in the x-direction, while the ramp rate dT/dt seen by the sample will be the product of its velocity v_x in the x-direction and the thermal gradient ΔT across the heater blocks.

3.3 Optical Setup

The optical access groove of the test rig is illuminated using a 473nm blue laser (Laserglow.com Ltd) which generates 80mW in a beam of 2mm diameter. The beam is expanded using PIV optics (Oxford Lasers Imaging Division). The beam is first expanded in the direction normal to the channel using a cylindrical lens (F=-50mm) and then expanded in the direction along the channel (F=-12.5mm). This generates a diffuse beam which is relatively uniform in the transverse direction but which is non-uniform in the direction along the channel.

The emission sensor used was a monochrome CCD camera (The Imaging Source). The CCD camera was filtered using a 515nm longpass filter (Melles-Griot). It was found that the detection system did not have sufficient sensitivity to detect fluorescence from samples when the entire channel (84mm) was used as the experimental field of view. However, focusing the camera on a field of view (FOV) of approximately 20mm provided sufficient resolution for measurements to be made. In order to have a sufficient temperature difference across the field of view to observe denaturation, the rig was operated at $T_c = 50°C$ and $T_h = 95°C$,

which produced a temperature difference within the field of view of $\Delta T_{FOV} \approx 10^{\circ}C$. This temperature field was determined by the efficiency of the cooling bath. During melting analysis, fluorescent measurements are typically made between $70^{\circ}C$ and $95^{\circ}C$ (10). However, *a priori* knowledge of the approximate t_m of the DNA fragment used permitted the selection of a temperature field such that the DNA sample denatured within the camera field of view [Fig 4]. In order to reduce the effect varying excitation intensity — a result of expanding the laser beam through a cylindrical lens — had on readings the excitation light was positioned such that the area of the FOV where higher temperatures were present (and hence where sample denaturation should occur) was subject to greatest illumination. This effect takes advantage of the higher quantum efficiencies of dsDNA dyes at lower temperatures.

4 EXPERIMENTAL PROCEDURE

The test rig is designed to analyse a serial of sample plugs buffered by mineral oil. The DNA sample is amplified using an ABI7900HT (Applied BioSystems) as described previously, and undergoes melting analysis in the same thermocycler to ensure product specificity. The sample is then aspirated into tubing (buffered by mineral oil) and this tubing is connected to the sample arm of the micro-fluidic T-junction (Upchurch Scientific) [Fig 3]. The sample is then pumped into the T-junction, while mineral oil is pumped into the carrier port at a greater flow rate (flow rate ratio 4:1). The carrier port generates a shearing force which shears fluid from the large sample plug, generating a series of small sample plugs within the flow leaving the outlet port. The volume of sample plugs varied due to imperfections in the T-junction and due to instability in the flow. The typical volume of plugs was $45nl$, but in some cases — where adjacent plugs merged — the volumes were was high as 500nl.

Due to the small field of view described above, the temperatures at which the test rig was operated was such that the temperature range within the field of view was approximately $10^{\circ}C$. Following the generation of sample plugs, the flow rates of the syringe pumps were reduced such that the ramp-rate seen by the plugs was $0.10^{\circ}C/s$, which is in line with that used in most commercial thermocyclers (10). As the samples traversed the test rig images were recorded while temperature data was logged using LabView (National Instruments).

5 MEASUREMENTS AND DATA ANALYSIS

Frame-grabbing software was used to acquire images of the optical access groove during the course of experimentation. An example of the typical image acquired, with two sample plugs in the field of view (located at approx 80pix and 220pix on the x-axis of image) is shown in Figure 5(a). Due to the location of the excitation light source, greater background noise can be seen in part of the image (approx 300pix to 600pix). Reflective artifacts, which could not be removed from the field of view, are also visible in the image.

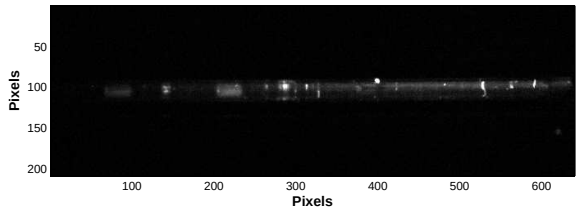

(a) Example of Typical Recorded Image

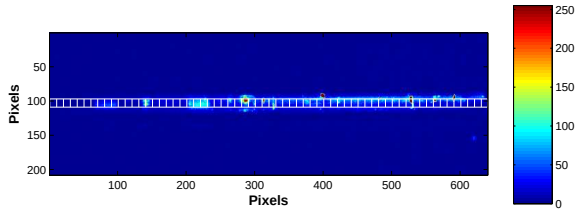

(b) Intensity Plot of Typical Recorded Image overlaid with Interrogation Areas.

Figure 5. Discrete Interrogation zones. Actual images recorded were 640x480 pixels. This image is cropped top and bottom for ease of plotting. Cropped areas were not of interest.

The images were analysed by dividing them into 64 interrogation zones. Each zone was 10 pixels wide and height equal to the width of the sample carrying channel. The mean intensity of each zone was then calculated, resulting in each image acquired being converted into 64 intensity measurements. The analysis areas can be seen overlaid upon Figure 5(b). Due to the large number of images acquired during experimentation — typically 3000 images were acquired during analysis of 30 sample plugs — the use of interrogation zones greatly reduced the computation required for data analysis. The presence of reflective artifacts resulted in a number of zones giving artificially high intensity readings. These interrogation zones are disregarded from the analysis.

As expected from the location of the excitation light source, the fluorescent of the sample increases greatly as it approaches the centre of the field of view. At higher temperatures — and as expected from denaturation of DNA samples — the fluorescence of samples attenuated to the background intensity. However, due to the variation in excitation light intensity along the optical access groove, the raw fluorescent signal from sample plugs did not resemble typical melting curves. Therefore, the fluorescent signal was normalised to account for its varying intensity.

The intensity of the excitation laser beam varied in its radial direction. This intensity variation is bell-shaped. The laser-beam is then expanded using a cylindrical lens. Hence, the

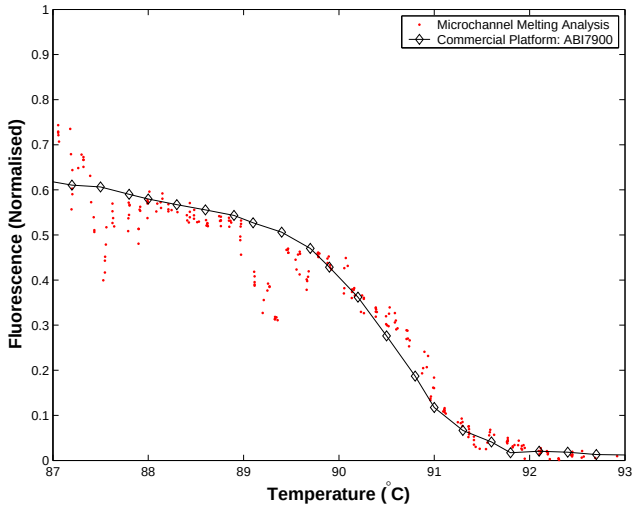

Figure 6. Comparison of DNA melting curves taken using commercial and microchannel platforms. The volume of the sample plug analysed in the microchannel platform is $98nl$

most intense light is along the laser centre-line. A plot of background noise in the field of view was generated by taking the mean intensity of each interrogation zone across all the frames recorded. This background noise distribution was approximately bell-shaped, and was assumed to be an indication of the excitation intensity each interrogation zone was subjected to. A line of best fit was passed through this background noise distribution, and this was used to normalise the raw fluorescent data.

Actual melt curves were generated from the fluorescent data by calculating, using logged temperature data and Equation 1, the temperature associated with the interrogation zone. The fluorescence intensity of an interrogation zone where a plug is present is then plotted against temperature; generating a melt curve for each plug observed.

6 RESULTS

A typical melt curve measured from the microchannel melting platform can be seen in Figure 6. It is compared with a melt-curve taken from the ABI7900 commercial thermal cycler. The data presented is scaled for comparison across different platforms. The data shows the same general trends as the commercial melt curve, with a drop in fluorescence associated with sample denaturation observed at approximately $90.5°C$. A deviation in the data presented from the commercial melt curve can be seen at $89.5°C$. This is a result of artifacts in the field of view. Greater scatter in normalised fluorescent readings was observed at lower temperatures. By design, this temperature range was subject to less illumination than the mid-range temperatures. However, this resulted in reduced robustness of the normalisation techniques when applied to these interrogation zones. This increased scatter was observed in almost all melt curves generated.

Due to the noise present in the data the melting peaks method — which involves differentiation of data — could not be applied to generate a denaturation temperature from the melting curves. Other techniques, such as that put forward by Gundry et al (14), could not be applied as a useable pre-denaturation baseline could not be generated from the small temperature window measured using this platform. In addition it can be observed in Figure 6 that data acquired, when plotted against temperature, bunches into discrete sets. This is a result of the interrogation zone approach taken to data analysis. This bunching of datapoints can make it difficult apply moving average smoothing. In view of this, the denaturation temperatures, t_m, from each curve was estimated by the user. In general, the denaturation temperatures were estimated at $90.9°C$ and measurements fell within a band of $\pm 1.0°C$.

The coalescence of some sample plugs resulted in measurements being made from plugs of different volumes. A number of sample plugs were analysed which were too small to produce useable melt curves. The minimum sample volume from which useful melting curves were generated was $45nl$. Melt curves were generated from samples as large as $500nl$. It was found that, within the observed accuracy of the test rig, variations in plug volume had no observable effect on t_m.

7 DISCUSSION AND CONCLUSION

The work describes in this paper demonstrates the ability to perform melting curve analysis upon a series of sample plugs buffered by an immiscible carried fluid. The platform demonstrates the capability to identify and distinguish homozygous PCR samples based upon t_m measurements. A device of this configuration has the advantage that the ramp-rate seen by the sample is a product of the thermal gradient applied to the device and the velocity of the sample through the test rig. Therefore, assuming the device is in a steady state varying the velocity of the sample varies its ramp rate. Although experiments performed in this paper were performed at $0.1°C$ the device is capable of operating at much lower ramp rates (hence resulting in greater $acq/°C$); limited only by the minimum flow rate from the syringe pump. Similarly, the steadiness of the ramp-rate is dependent on the steadiness of the flow from the syringe pump.

The experimental platform was used to measure the denaturation temperatures of samples of varying volumes. The minimum volume detectable by this test rig was $45nl$. Within the accuracy of the test rig, the length or volume of the sample plugs had no effect upon the denaturation temperatures t_m observed. This infers that the recirculation which may occur within these plugs has no effect upon the thermal development of the flow.

The performance of the experimental rig suffered from the inefficiency of the optical set up used. The use of a non-

uniform excitation light allowed homozygous t_m measurements be made. However, the rig in this configuration would not be capable of multiplex PCR analysis or heterozygous melting analysis (12; 14; 17) as these techniques require accurate measurement of the shape of the melt curve rather than just measurement of the denaturation temperature t_m. In addition, the optical set up limited the temperature window which was measured, and this in turn limited the computational algorithms which could be applied to the data.

There are a number of alternative approaches possible to remove the limitations from the test rig. The inclusion of a reference dye into each sample plug, and the use of a second sensor to measure this intensity would allow accurate normalisation of fluorescent readings. Reducing the length of the test device would make it easier to illuminate it with uniform light from a single light source. Miniaturisation would offer alternative challenges, such as the tendency of small devices to become isothermal. However, advances in micro-channel heat transfer may make this feasible in the future. Another alternative would be to use other heating techniques, such as placing a substrate on a heat sink and applying ohmic heating directly to the substrate (15). We surmise that correct design of such ohmic heating might allow a linear thermal gradient be generated along a curved or serpentine channel, further decreasing the size of a miniaturised device. A further approach would be to use multiple calibrated light source/sensor pairs along the channel to make a discrete number of measurements.

As fluorimeters were integrated into traditional PCR thermocyclers and made quantitive PCR (qPCR) possible, it is clear that the next step in the development of flowing PCR thermocyclers on the micro-scale will be the integration of some manner of fluorescent detection (19; 20). Well-based melting curve analysis offers a simple, closed tube addition to the well-based PCR thermocycler for applications in quality control, multiplexing and SNP detection; similarly microchannel melting analysis has the potential to be integrated into flowing PCR thermocycler systems and can offer much the same functionality.

REFERENCES

[1] Bertucci, F., Houlgate, R., Nguyen, C., Viens, P., Jordan, B., and Birnbaum, D., 2001. "Gene expression profiling of cancer by use of DNA arrays: how far from the clinic?". *The Lancet Oncology,* **2** , pp. 674–682.

[2] Golub, T., Slonim, D., Tamayo, P., Huard, C., Gaasenbeek, M., Mesirov, J., Coller, H., Loh, M., Downing, J., Caligiuri, M., Bloomfield, C., and Lander, E., 1999. "Molecular Classification of Cancer: Class Discovery and Class Prediction by Gene Expression Monitoring". *Science,* **286** , pp. 531–537.

[3] Abruzzo, L., Lee, K., Fuller, A., Silverman, A., Keating, M., Medeiros, L., and Coombes, K., 2005. "Validation of oligonucleotide microarray data using microfluidic low-density arrays: a new statistical method to normalise real-time RT-PCR data". *Biotechniques,* **38** , pp. 785–792.

[4] Wong, M., and Medrano, J., 2005. "Real-time PCR for mRNA quantitation". *Biotechniques,* **39** , pp. 75–85.

[5] Stahlberg, A., Zoric, N., Aman, P., and Kubista, M., 2005. "Quantitative real-time PCR for cancer detection: the lymphona case". *Expert Review in Molecular Diagnostics,* **5** , pp. 221–230.

[6] Howbrook, D., van der Valk, A., O'Shaughnessy, M., Sarker, D., Baker, S., and Lloyd, A., 2003. "Developments in microarray technologies". *Drug Discovery Today,* **8** , pp. 642–651.

[7] Erikson, D., and Li, D., 2004. "Integrated microfluidic devices". *Analytica Chimica Acta,* **507** , pp. 11–26.

[8] Schneegass, I., and Kohler, J., 2001. "Flow-through polymerase chain reactions in chip thermocyclers". *Reviews in Molecular Biotechnology,* **82** , pp. 101–121.

[9] Wittwer, C., Herrmann, M., Moss, A., and Rasmussen, R., 1997. "Continuous fluorescence monitoring of rapid cycle DNA amplification". *Biotechniques,* **22** , pp. 130–138.

[10] Herrmann, M. G., Durtschi, J. D., Bromley, L. K., Wittwer, C. T., and Voelkerding, K. V., 2006. "Amplicon DNA Melting Analysis for Mutation Scanning and Genotyping: Cross-Platform Comparison of Instruments and Dyes". Clinical Chemistry, **52** (3) , pp. 494–503.

[11] Zhou, L., Myers, A., Vandersteen, J., Wang, L., and Wittwer, C., 2004. "Closed-tube genotyping with unlabeled oligonucleotide probes and a saturating DNA dye". Clinical Chemistry, **50** (8) , pp. 1328–1335.

[12] Hernandez, M., Rodriquez-Lazaro, D., Esteve, T., Prat, S., and Pla, M., 2003. "Development of melting temperature based SYBR Green I polymerase chain reaction methods for multiplex genetically modified organism detection". *Analytical Biochemistry,* **323** , pp. 164–170.

[13] Hiratsuka, M., Narahara, K., Kishikawa, Y., Hamdy, S., Endo, N., Agatsuma, Y., Matsuura, M., Inoue, T., Tomioka, Y., and Mizugaki, M., 2002. "A simlultaneous LightCycler detection assay for five genetic polymorphisms influencing drug sensitivity". *Clinical Biochemistry,* **35** , pp. 35–40.

[14] Gundry, C., Vandersteen, J., Reed, G., Pryor, R., Chen, J., and Wittwer, C., 2003. "Amplicon Melting Analysis with Labled Primers: A Closed-Tube Method for Differentiating Homozygotes and Heterozygotes". Clinical Chemistry, **49** (3) , pp. 396–406.

[15] Cibuzar, G., Fisher, M., Williamson, F., Blumenfeld, M., Suntharalingam, P., Grenz, J. R., Ness, B. G. V., Kim, K. J., Bar-Cohen, A., and Eccleston, E., 2003. "Development of a New Technique for DNA Single Base Pair Mismatch Analysis". In Proceedings of the 15th Biennial University/Government/Industry Microelectronics Symposium, IEEE, pp. 184–194.

[16] Mao, H., Holden, M. A., You, M., and Cremer, P. S., 2002. "Reusable Platforms for High-Throughput On-Chip Temperature Gradient Assays". *Analytical Chemistry,* **71** , pp. 5071–5075.

[17] Sundberg, S. O., Wittwer, C. T., Greer, J., Prior, R. J., Elintoba-Johnson, O., and Gale, B. K., 2007. "Solution-phase DNA mutation scanning and SNP genotyping by nanoliter melting analysis". Biomedical Microdevices, **9** (2) April , pp. 159–166.

[18] Dalton, T. M., Kinahan, D. J., and Davies, M. R., 2005. "Fluorescent Melting Curve Analysis compatible with a Flowing Polymerase Chain Reactor". In Proceedings of 2005 ASME International Mechanical Engineering Congress and Exposition, ASME.

[19] Sayers, M. B., Dalton, T. M., and Davies, M. R., 2006. "Real-Time Fluorescence Monitoring of the Polymerase Chain Reaction in a Novel Continuous Flow Reactor for Accurate DNA Quantification". In Proceedings of 4th International Conference on Nanochannels, Microchannels and Minichannels, ASME.

[20] Chabert, M., Dorfman, K. D., de Cremoux, P., Roeraade, J., and Viovy, J.-L., 2006. "Automated Microdroplet Platform for Sample Manipulation and Polymerase Chain Reaction". *Anal Chem,* **78** , pp. 7722–7728.